RSC Advances

PAPER

View Article Online
View Journal | View Issue

Cite this: *RSC Adv.*, 2017, **7**, 11403

Synthesis of magnetic carbonaceous acids derived from hydrolysates of *Jatropha* hulls for catalytic biodiesel production†

Fan Zhang,‡*[ad] Xiaofei Tian,‡[b] Mazloom Shah[ac] and Wenjing Yang[a]

A series of magnetic carbonaceous acids (JHC-T_1–T_2-SO_3H@Fe/Fe_3O_4) were synthesized by the assembly of nano-Fe_3O_4 magnetic cores (particle size < 20 nm) and carbon coatings derived from hydrolysates of *Jatropha* hulls. A magnetic JHC-12-600-SO_3H@Fe/Fe_3O_4 catalyst with a total acid content of 2.69 mmol g^{-1} and a magnetic saturation of 40.3 A m^2 kg^{-1} was successfully prepared *via* a sequence of hydrothermal precipitation, pyrolytic carbonization, and finally sulfonation with H_2SO_4. The catalyst was directly used for the production of biodiesel from *Jatropha* crude oil with an acid value (AV) of 17.2 mg KOH per g, and the optimized conditions (180 °C for 7.5 h with a molar ratio of methanol/oil of 18/1 and a catalyst loading of 7.5 wt%) were determined by single-factor tests. An average biodiesel yield of 95.9% was achieved with a recovery rate of 94.3% after 5 reaction cycles in a 5 L batch reactor for testing the feasibility of the catalyst for large-scale use. This study demonstrates an alternative green approach to fully utilizing waste biomass from energy plants in the catalytic synthesis of *Jatropha* biodiesel with high efficiency.

Received 29th December 2016
Accepted 31st January 2017

DOI: 10.1039/c6ra28796d

rsc.li/rsc-advances

1. Introduction

Limitations in fossil oil reserves and global warming have become serious problems because of the growing global demand for energy and the accumulation of atmospheric CO_2 by the combustion of fossil fuels.[1,2] Biodiesel is considered to be an alternative liquid fuel owing to the advantage that it is clean and renewable.[3,4] Because heterogeneous catalysts are easier to recover from the reaction system than liquid acid or alkaline catalysts,[5] solid catalysts have been widely employed in the production of biodiesel. Solid basic catalysts including K/SiO_2,[6] CaO from eggshells[7] and calcium-modified porous aluminosilicates[8] have commonly been used in the production of biodiesel owing to their high performance in transesterification reactions of oils with a low acid value (AV). Natural *Jatropha* oil is a promising raw material for the production of biodiesel with suitable properties.[9–11] However, it always has a high AV, which is caused by long-term storage.[12,13] To avoid the direct use of basic catalysts, which would cause severe saponification of the reaction system during the transesterification of *Jatropha* oil, deoxygenation of fatty acids[14] and transesterification with enzyme[15] or solid acid catalysts[16–18] are effective methods that have been widely employed in the production of biodiesel. However, deficiencies in these methods, such as the high cost of lipases, harsh deoxygenation conditions and incomplete separation of the catalyst particles from the products, remained and posed challenges to their further utilization in the large-scale production of biodiesel.[14–18]

When catalyzing hydrolysis, esterification and dehydration reactions, solid acid catalysts, in particular sulfonated solid acid catalysts, exhibited excellent performance in the conversion of various alternative carbon resources, such as lignocellulosic biomass,[19] sugars,[20] and non-edible oils,[21,22] for the purposes of producing fuels and high-value-added chemicals. For example, sulfated mesoporous niobium oxide (MNO-S) was developed as a catalyst for the production of 5-hydroxymethylfurfural (5-HMF). It catalyzed the hydrolysis and dehydration reactions of various disaccharide substrates and exhibited promising feasibility owing to a relatively high yield of 5-HMF and excellent recyclability.[20]

As sulfonated active carbon has been successfully employed in the catalytic production of biodiesel from crude *Jatropha* oil with a high AV of 12.7 mg KOH per g,[22,23] the efficient recycling of solid carbons is of key importance for the purpose of reusing catalysts. Centrifugation and filtration methods have been commonly used, but both of them operated with low time or energy efficiency.[22] The introduction of a magnetic field for the

[a]*Biomass Group, Key Laboratory of Tropical Plant Resources and Sustainable Use, Xishuangbanna Tropical Botanical Garden, Chinese Academy of Sciences, 88 Xuefulu, Kunming, Yunnan, 650223, China. E-mail: zhangfan@xtbg.ac.cn; Web: http://www.tprsu.xtbg.ac.cn/; Fax: +86-871-65160916; Tel: +86-871-65180637*

[b]*School of Bioscience and Bioengineering, South China University of Technology, University Mega Centre, Guangzhou, Guangdong, 510006, China. E-mail: xtien@scut.edu.cn*

[c]*Department of Chemistry, Women University of Azad Jammu and Kashmir, Bagh, 12500, Pakistan. E-mail: shahmazloom@gmail.com*

[d]*University of Chinese Academy of Sciences, 19A Yuquan Road, Beijing, 100049, China*

† Electronic supplementary information (ESI) available. See DOI: 10.1039/c6ra28796d

‡ Co-first authors.

isolation of catalysts from the reaction system was a practical approach without intensive consumption of time or energy. Magnetic carbonaceous acids provided a convenient way of using a magnet for the isolation of catalysts. Novel carbon-based materials, including sulfonated magnetic lignin-derived amorphous carbon solid acids (MLC-SO_3H),[24] magnetic carbon nanotube arrays (sulfonated MCNAs)[25] and magnetic carbonaceous acids,[19,26,27] were synthesized and successfully used in catalyzing the dehydration of fructose and the hydrolysis of polysaccharides and cellulose, respectively. However, these reported magnetic carbonaceous acids were not adequate for employment in the production of biodiesel with high efficiency owing to their relatively low acidity or magnetism (Table 1).

In our previous work,[28] an alternative magnetic AC-600-SO_3H@Fe/C catalyst with high acidity and magnetic saturation was synthesized using glucose as the source of the carbon coating. With remarkably high efficiency in the transesterification of *Jatropha* oil and a high catalyst recovery rate, it was successfully employed for the production of *Jatropha* biodiesel. As the synthesis of the catalyst required edible sugar and complicated operations (Table 1), we therefore developed

Table 1 Preparation, acid content and magnetism of selected magnetic carbonaceous acids

Catalyst	Raw materials	Preparation methods	Acidity (mmol g^{-1})	Magnetism (A m^2 kg^{-1})	Catalytic reaction	Ref.
MLC-SO_3H	Residue of enzymatic hydrolysis of corn stover and $FeCl_3$	Mixture: (300 rpm, 5 h); impregnation: (65 °C, 12 h); pyrolysis: (400 °C, 1 h); sulfonation: (150 °C, H_2SO_4, 10 h)	1.95[a]		Dehydration of fructose to 5-hydroxymethylfurfural	24
Sulfonated MCNAs	Xylene and ferrocene	Pyrolysis: (800 °C; the solution was injected by a syringe pump at a rate of 0.05 mL min^{-1} for 2 h with a flow rate of 60 sccm H_2 and 400 sccm ar); sulfonation: (250 °C, H_2SO_4, 18 h)	0.38[b]	6.32[c]	Hydrolysis of polysaccharides in crop stalks	25
C–SO_3H/Fe_3O_4	Glucose and Fe_3O_4	Agitation: (Fe_3O_4 and glucose solution, 100 °C, about 10 h); calcination: (700 °C, 1 h); sulfonation: (150 °C, H_2SO_4, 19 h)	0.75[a]	19.5	Hydrolysis of cellulose to glucose	19
C–SO_3H/Fe_3O_4@	Glucose and $FeCl_3$	Hydrothermal carbonization: (glucose 180 °C, 14 h); desiccation: (40 °C, 12 h); sulfonation: (60 °C, H_2SO_4, 24 h)	1.30[a]	23	Hydrolysis of cellulose to glucose	26
PMC-SO_3H	Cellulose and Fe_3O_4	Hydrothermal carbonization: (cellulose 250 °C, 14 h); desiccation: (80 °C, 12 h); agitation: [$Fe(NO_3)_3$ and NH_3 solution, 250 °C, 24 h]; sulfonation: (80 °C, *p*-toluenesulfonic acid, 12 h); calcination: (400 °C, 12 h)	0.64[d]	4.71	Hydrolysis of cellulose to glucose	27
SO_3H–Fe/C	Glucose and $FeCl_3$	Hydrothermal precipitation: (180 °C, 14 h); pyrolysis: (700 °C, 1.5 h); sulfonation: (150 °C, H_2SO_4, 16 h)	1.67[b]	0.43	—	28
AC-600-SO_3H@ Fe/C	Glucose and $FeCl_3$	Hydrothermal precipitation: (180 °C, 14 h); pyrolysis: (700 °C, 1.5 h); hydrothermal coating: (180 °C, 14 h); pyrolysis: (600 °C, 1.5 h); sulfonation: (150 °C, H_2SO_4, 16 h)	2.79[b]	14.4	Transesterification of crude *Jatropha* oil with high AV	28
JHC-12-600-SO_3H@Fe/Fe_3O_4	Hydrolysates and Fe_3O_4	Hydrothermal precipitation: (180 °C, 12 h); pyrolysis: (600 °C, 1.5 h); sulfonation: (180 °C, 12 h)	2.69[b]	40.3	Transesterification of crude *Jatropha* oil with high AV (17.2 mg KOH per mg)	Present work

[a] By acid–base titration. [b] By NH_3-TPD analysis. [c] Before sulfonation. [d] Calculated on the assumption that all the sulfur atoms were associated with sulfonic acid groups.

a method for preparing a series of magnetic carbonaceous acids *via* hydrothermal precipitation, pyrolytic carbonization and sulfonation using nano-Fe_3O_4 particles and hydrolysates of *Jatropha* hulls as alternative raw materials. The prepared magnetic carbonaceous acid that had the highest acidity and a relatively high magnetic saturation was selected and employed for the production of *Jatropha* biodiesel under conditions optimized by single-factor experiments.

2. Experiments

2.1. Materials

Nano-Fe_3O_4 particles (≥99.5%, particle size < 20 nm) were purchased from Aladdin Industrial Corporation (Shanghai, China). Analytical reagents, namely, concentrated H_2SO_4 (≥98.0%), $Ca(OH)_2$ (≥95.0%), methanol (≥99.5%), KOH (≥85.0%), dehydrated ethanol (≥99.5%) and phenolphthalein were purchased from Xilong Chemical Factory Co., Ltd. (Shantou, Guangzhou, China). Standard materials of heptadecanoic acid methyl ester ($C_{17:0}$) and other aliphatic acid methyl esters [palmitate ($C_{16:0}$), palmitoleate ($C_{16:1}$), stearate ($C_{18:0}$), oleate ($C_{18:1}$), linoleate ($C_{18:2}$) and linolenate ($C_{18:3}$)] (≥99.0%) were purchased from Sigma-Aldrich (Shanghai, China).

Jatropha hulls were purchased from Yunnan Shenyu New Energy Co., Ltd. (Chuxiong, Yunnan, China). Before use, they were dried at 75 °C for 48 h and ground to pass through a sieve (80 mesh) using a pulverizer (9FC15, Xudong Machinery Manufacturing Co., Ltd, Leshan, Sichuan, China). Elemental analysis of the *Jatropha* hulls was performed using an elemental analyzer (Vario EL III CHNS, Elementar Analysensysteme GmbH, Hanau, Germany). The contents of C, H and O were 48.6%, 7.23% and 41.1% wt, respectively (Table 2). For acid hydrolysis, 15 g *Jatropha* hulls were loaded in a 300 mL ZrO_2 reactor (FCFD03-30, Jianbang Chemical Mechanical Co. Ltd, Yantai, Shandong) containing 200 mL of 3 wt% concentrated H_2SO_4 solution. The suspension was thoroughly mixed by stirring at 300 rpm and heated to 150 °C. After 1.5 h, the reactor was cooled immediately. The residue of *Jatropha* hulls was removed by passing them through a filter (Merck Millipore, pore size 1.2 μm), and the hydrolysates were neutralized by adding $Ca(OH)_2$ until the pH was 6.5–7.0. After filtration, the hydrolysates were further concentrated at 65 °C in a rotary evaporator (RE-52AA, Yancheng Instrument Co., Ltd, Shanghai, China). A concentration of soluble carbon of 61 g L^{-1} in the hydrolysates was finally achieved. Crude *Jatropha* oil (stored for six years) was obtained from Xishuangbanna Tropical Botanical Garden, Chinese Academy of Sciences.

2.2. Catalyst preparation

Firstly, 20 g nano-Fe_3O_4 particles (magnetic cores) were loaded into a 500 mL ZrO_2 reactor (FCFD05-30, Jianbang Chemical Mechanical Co., Ltd, Yantai, Shandong, China) containing 0.4 L concentrated hydrolysates of *Jatropha* hulls. The mixture was maintained at 180 °C for different hydrothermal precipitation times (4, 8, 12, 16 and 20 h) while being stirred at 500 rpm. After the hydrothermal reaction, the solid product was recovered and washed with deionized water several times until a neutral solution was obtained. The neutralized solid product was saturated with dehydrated ethanol and freeze-dried at −47 °C in a freeze-dryer (PDU-1200, EYELA, Tokyo Rikakikai Co., Ltd, Japan) for 24 h. Carbonization of the magnetic carbonaceous precursor was performed in a tubular furnace (SGL-1100, Daheng Optics and Fine Mechanics Co., Ltd, Shanghai, China) with a nitrogen flow of 200 mL min^{-1}. The temperatures in the oven reached 200, 400, 500, 600, 700 and 800 °C with a heating rate of 1.9–8.6 °C min^{-1} for 1.5 h. The products were designated as JHC-T_1–T_2@Fe/Fe_3O_4 (T_1 is the hydrothermal precipitation time, T_2 is the temperature of pyrolytic carbonization), respectively.

A 10 g sample of JHC-T_1–T_2@Fe/Fe_3O_4 was added to a 500 mL flask containing 200 mL concentrated H_2SO_4. The mixture was maintained at 180 °C for 12 h under a nitrogen flow (100 mL min^{-1}). The sulfonated JHC-T_1–T_2@Fe/Fe_3O_4 (JHC-T_1–T_2-SO_3H@Fe/Fe_3O_4) that was obtained was washed with hot distilled water (70–80 °C) until the pH was 6.5–7. To remove the residual SO_4^{2-}, the neutralized JHC-T_1–T_2-SO_3H@Fe/Fe_3O_4 was hydrothermally treated with water at 180 °C for 3 h in the reactor. The treated JHC-T_1–T_2-SO_3H@Fe/Fe_3O_4 was washed and freeze-dried. Before being used for the production of biodiesel, the prepared catalyst was ground and sieved through a 200 mesh screen.

2.3. Instrumentation

The total acid content (TAC) was measured by the temperature-programmed desorption (TPD) method using a chemisorption analyzer (Quantachrome Instruments, Boynton Beach, FL,

Table 2 Elemental compositions (C, H, N, S and Fe) of *Jatropha* hulls, the magnetic JHC-12-600@Fe/Fe_3O_4 precursor and the magnetic JHC-12-600-SO_3H@Fe/Fe_3O_4 catalyst

Wt%	*Jatropha* hulls	JHC-12-600@Fe/Fe_3O_4	JHC-12-600-SO_3H@Fe/Fe_3O_4	JHC-12-600-SO_3H@Fe/Fe_3O_4[d]
C[a]	48.6	35.1	40.7	41.5
H[a]	7.23	3.88	2.27	2.44
O[b]	41.1	16.2	32.5	—
N[a]	2.67	1.67	1.11	0.82
S[a]	0.173	0.250	3.62	2.37
Fe[c]	0.227	42.9	19.8	—

[a] Analyzed by Vario EL III CHNS elemental analyzer. [b] O (wt%) was calculated as 100 wt% – (C, H, N, S, and Fe) wt%. [c] Analyzed by ICP-OES. [d] JHC-12-600-SO_3H@Fe/Fe_3O_4 catalyst after 5 cycles of use.

USA). About 50–100 mg of the catalyst was used for TPD analysis. The program used for the reacting gas and sample temperature was as follows: standard gas (10% NH_3 with 90% He, v/v, Yunnan Messer Co., Ltd, Kunming, China) was supplied for 60 min at 50 °C at a flow rate of 85 mL min^{-1} and then converted to He gas (99.999%, Yunnan Messer Co., Ltd, Kunming, China), and the temperature was gradually increased to 400 °C at a heating rate of 5 °C min^{-1} over 60–90 min. The total acid content was calculated using an external standard, which was calibrated against 0.5, 1, 1.5, and 2 mL of a standard gas (10% NH_3 with 90% helium). Saturation magnetization (Ms) was measured using a vibrating sample magnetometer (VSM; Lake Shore 7407, Lake Shore Cryotronics, Inc., Westerville, OH, USA). Crystal structures were determined using an X-ray diffractometer (XRD; Rigaku Rotaflex RAD-C, Tokyo, Japan) equipped with a Cu Kα radiation source. All samples were equally loaded. The composition of metallic oxides in the catalyst was determined according to a pairwise comparison of diffraction patterns with standard records (Joint Committee on Powder Diffraction Standards, JCPDS: 89-2355, 06-0696, 72-1110 and 39-1346).[29] The surface morphologies and microstructures of the catalysts and precursors were characterized using a scanning electron microscope (SEM; Zeiss EVO LS10, Cambridge, UK). The samples were loaded on copper mounts with double-sided electrically conductive adhesive carbon tape without gold coatings. Observations with the SEM were conducted using an accelerating voltage of 10.00 kV at a working distance of 15.5 mm. Transmission electron microscopy (TEM) images were recorded using a JEOL JEM-2010 microscope at an accelerating voltage of 200 kV. A suspension of the catalyst or precursor, which had been well dispersed in ethanol by ultrasonication, was dropped onto the copper grid and air-dried before being subjected to observation. Surface areas were selected and scanned by energy-dispersive X-ray spectrometry (EDX; Quanta 200, Hillsboro, OR, USA) for the determination of semi-quantitative elemental compositions (C, O, Fe and S). Functional groups were identified by Fourier transform infrared spectroscopy (FT-IR; Nicolet iS10, Thermo Fisher Scientific Co., Ltd, Waltham, MA, USA) within the spectral range of 400–4000 cm^{-1}. A 0.05 g freeze-dried sample was blended with 0.5 g spectroscopic grade KBr in an agate mortar and then pressed into a disc. The KBr disc was scanned with a resolution in the range of 0.4–4 cm^{-1}. The thermal stability of samples was determined using a thermogravimetric analyzer (TGA; TA Q500 HiRes, TA Instruments, New Castle, DE, USA). With 5 mg freeze-dried catalyst loaded in the TGA crucible, data were collected at temperatures rising from 40 to 800 °C at 5 °C min^{-1} under a helium gas atmosphere flowing at 50 mL min^{-1}. The Brunauer–Emmett–Teller (BET) surface area and pore volume were measured by the nitrogen adsorption–desorption method using a TriStar II 3020 (Micromeritics Instrument Co., Ltd, Norcross, GA, USA). The samples were degassed at 120 °C for 3 h before analysis. The elemental composition was determined using an elemental analyzer (Vario EL III CHNS, Elementar Analysensysteme GmbH, Hanau, Germany). The catalysts were dissolved in an oxidizing agent containing 10% HCl and 3.5% HNO_3 (w/w). The Fe content was determined by an inductively coupled plasma-optical emission spectrometer (ICP-OES; Optima 5300 DV, PerkinElmer Inc., Waltham, MA, USA).

2.4. Biodiesel production and catalyst recovery

The catalytic esterification and transesterification of crude *Jatropha* oil were performed in a 50 mL batch reactor (YZPR-50, Yanzheng Experimental Instrument Co., Ltd, Shanghai, China) equipped with a quartz cup (Fig. 1). With a dead volume of 9.6 mL, the sealed reactor containing 18.6 g (0.02 mol) crude *Jatropha* oil, methanol (in a molar ratio to the oil of 6 : 1–30 : 1) and the catalyst (2.5–12.5 wt% of the oil) was pressurized with nitrogen (2.0 MPa, 99.99%, Yunnan Messer Co., Ltd, Kunming, China) to avoid the evaporation of methanol at high temperatures. The reaction was conducted at 160–200 °C with a heating time of 25–35 min allowed before reaching the reaction temperature. After the reaction, the catalyst was isolated from the liquid using an NdFeB magnet (Fig. 1c) and subjected to direct reuse without any treatment.

The large-scale production of *Jatropha* biodiesel in a 5 L batch reactor (FCFD05-30, Jianbang Chemical Mechanical Co., Ltd, Yantai, Shandong, China) with a dead volume of 36.7 mL (Fig. 2) was performed over the selected catalyst under conditions optimized *via* small-scale experiments. Before the reaction, an appropriate amount of the magnetic catalyst was first loaded on an NdFeB magnet fixed on the mixer shaft (Fig. 2b). Crude *Jatropha* oil (1.86 kg, 2 mol) and methanol were pumped into the reactor, which was sealed and then pressurized with nitrogen (99.999% purity, 2.0 MPa). High-speed stirring at 500 rpm was applied to homogenize the mixture with the catalyst. Then the

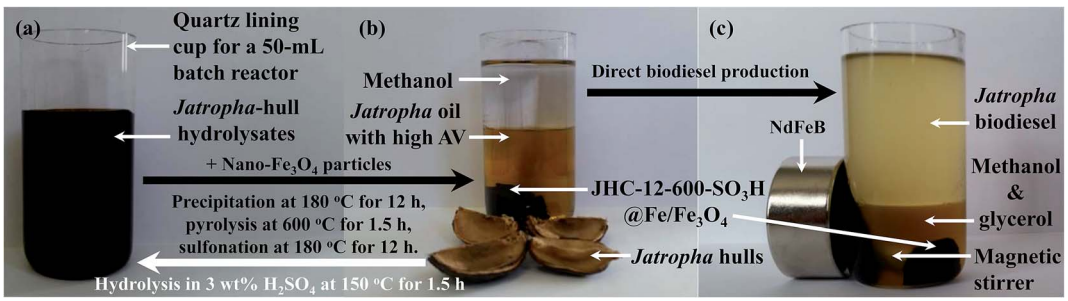

Fig. 1 Images of (a) hydrolysates of *Jatropha* hulls, (b) a mixture of magnetic JHC-12-600-SO_3H@Fe/Fe_3O_4 with *Jatropha* oil and methanol in a 50 mL batch reactor, and (c) the catalyst recovered by an NdFeB magnet from the synthesized *Jatropha* biodiesel.

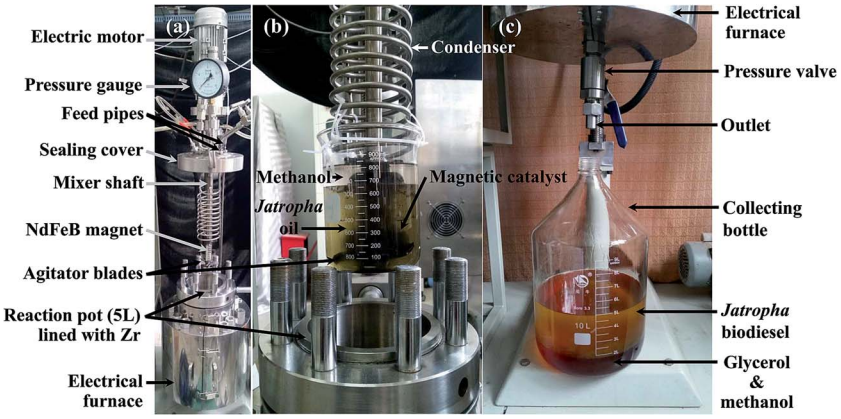

Fig. 2 Images of (a) the 5 L batch reactor used for the production of biodiesel, (b) the magnetic JHC-12-600-SO_3H@Fe/Fe_3O_4 catalyst attracted by the NdFeB magnet, which was attached to the mixer shaft, and (c) *Jatropha* biodiesel, glycerol and methanol pumped out of the reactor.

reactor was heated to 180 °C within 60 min. After the reaction, the reactor was immediately cooled using circulating water for 0.5–1 h. The products were discharged slowly through the outlet valve (Fig. 2c), and the magnetic catalyst was collected on the mixer shaft attached to the NdFeB magnet for reuse.

After 3 cycles, the recycled catalyst was washed with an adequate amount of dehydrated ethanol 3–5 times and dried at 105 °C until a consistent weight was reached for calculation of the catalyst recovery rate.

$$\text{Catalyst recovery (wt\%)} = (\text{mass of recovered catalyst, g})/(\text{mass of fresh catalyst, g}) \times 100\% \quad (1)$$

2.5. Biodiesel assays

The AV (17.2 mg KOH per g) and saponification value (SV, 195.7 mg KOH per g) of the crude *Jatropha* oil samples were measured according to national standard protocols (GBT 5530-2005 and 5534-2008). The calculated average molecular weight of the crude oil was 942.9 g mol^{-1} according to the formula [$M = (56.1 \times 1000 \times 3)/(SV - AV)$].[30]

The crude biodiesel that was produced was first clarified by being passed through a filter (pore size 0.22 μm, Merck Millipore). A Shimadzu gas chromatography (GC) system (GC-2014, Kyoto, Japan) equipped with a capillary column (Rtx-Wax, 30 m × 0.25 mm × 0.25 μm, Restek Corporation, Bellefonte, PA, USA) and a flame ionization detector (FID) was used for quantitative analysis of the yield of methyl esters in the product. Helium (99.999%) was used as the carrier gas at a flow rate of 1 mL min^{-1}. A 10 μL sample was injected with a split ratio of 40 : 1. The temperatures of the column, injector and detector were maintained at 220, 260 and 280 °C, respectively.

The amount of methyl esters was calculated using $C_{17:0}$ as an internal standard. The yield of biodiesel was calculated by the equation reported in our previous work.[30]

$$\text{Biodiesel yield (wt\%)} = \{[(A_{C16:0}/f_{C16:0} + A_{C16:1}/f_{C16:1} + A_{C18:0}/f_{C18:0} + A_{C18:1}/f_{C18:1} + A_{C18:2}/f_{C18:2} + A_{C18:3}/f_{C18:3} + A_{Cothers})/A_{C17:0}] \times \text{weight of } C_{17:0}\}/(\text{weight of crude biodiesel}) \times 100\% \quad (2)$$

where A_{Cn} (n = 16 : 0, 16 : 1, 18 : 0, 18 : 1, 18 : 2, and 18 : 3) is the peak area for the six standard methyl esters ($C_{16:0}$, $C_{16:1}$, $C_{18:0}$, $C_{18:1}$, $C_{18:2}$, and $C_{18:3}$), $A_{Cothers}$ is the peak area for the other components except A_{Cn}, and f_{Cn} (1.014, 1.023, 1.076, 1.038, 1.019, and 0.926) is the relative response factor of C_n to that of $C_{17:0}$.[31]

3. Results and discussion

3.1. Synthesis of magnetic carbonaceous acids

3.1.1. Reaction time for hydrothermal precipitation. The different reaction times used in the hydrothermal precipitation (between 4 and 20 h) of the magnetic carbonaceous precursors (JHC-T_1–600@Fe/Fe_3O_4) were optimized with respect to the TAC and Ms of the final acid catalyst. After sulfonation at 180 °C for 12 h, the TAC and Ms of the JHC-T_1–600-SO_3H@Fe/Fe_3O_4 catalyst increased sharply from 0.290 mmol g^{-1} and 10.3 A m^2 kg^{-1} to 1.80 mmol g^{-1} and 26.3 A m^2 kg^{-1}, respectively, as the reaction time increased from 4 to 8 h (Fig. 3a). When the reaction time was further increased to 12 h and then to 20 h, the Ms decreased from a maximum value of 40.3 A m^2 kg^{-1} to 34.4 A m^2 kg^{-1}, but the TAC continuously increased from 2.69 mmol g^{-1} to 3.01 mmol g^{-1}.

With an increase in the hydrothermal precipitation time, the increase in the loading capacity of JHC-4-600@Fe/Fe_3O_4 for –SO_3H groups was attributed to the growth in the carbonaceous surface areas of the magnetic cores *via* the continuous deposition of bulk carbon derived from the hydrolysates. SEM and TEM images (Fig. 4A-a and b) showed that a short precipitation time (4 h) led to a defective carbonaceous layer on the JHC-4-600@Fe/Fe_3O_4 precursor, which failed to protect the magnetic cores from corrosion by H_2SO_4 during sulfonation. EDX analysis (Fig. 4A-c) revealed that the carbon content was lower (6.60 wt%) in comparison to that of O (22.6 wt%) or Fe (70.8 wt%) on the surface of the precursor. After hydrothermal precipitation for 20 h, a complete carbonaceous coat was observed on JHC-20-600-SO_3H@Fe/Fe_3O_4 (Fig. 4B-a and b). The C and S contents (wt%) that were determined significantly increased to 33.1 and 21.4, respectively, whereas the O and Fe contents decreased to 18.6 and 26.9, respectively (Fig. 4B-c). However, the overloaded

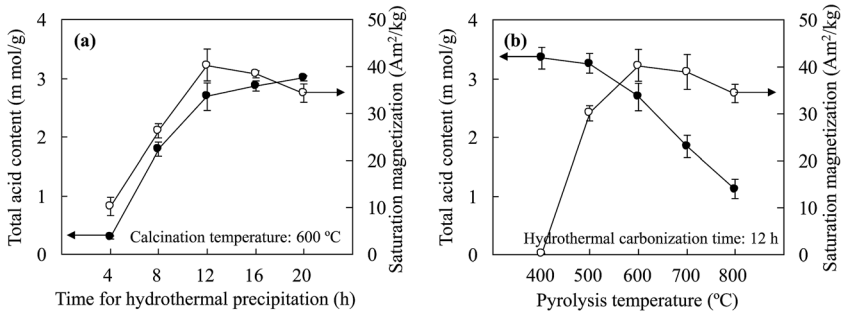

Fig. 3 Changes in the total acid content and saturation magnetization of the prepared solid acids *versus* (a) the hydrothermal precipitation time and (b) the carbonization temperature used in synthesis of the catalyst precursor.

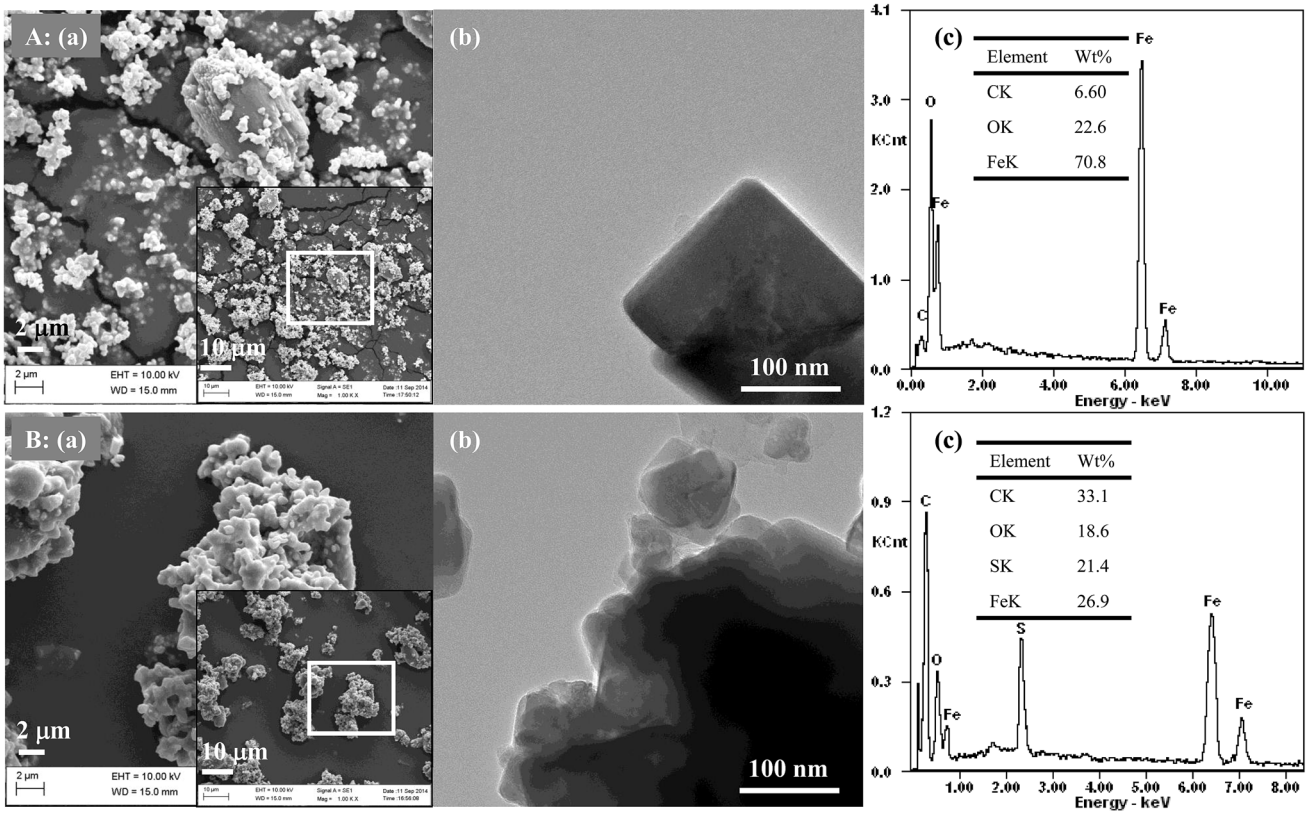

Fig. 4 Observations of the surface morphologies and microstructures of the catalyst and catalyst precursor: (a) SEM images, (b) TEM images and (c) EDX spectra of (A) the magnetic JHC-4-600@Fe/Fe_3O_4 precursor and (B) the magnetic JHC-20-600-SO_3H@Fe/Fe_3O_4 catalyst.

carbonaceous coat decreased the relative content of magnetic Fe_3O_4 in the catalyst and thus led to a slight reduction in the Ms. In this study, 12 h was selected as the best hydrothermal precipitation time for preparing the catalyst in the following experiments.

3.1.2. Carbonization temperature. Different temperatures were selected for the carbonization of the catalyst precursor JHC-12–T_2@Fe/Fe_3O_4 of between 400 and 800 °C (Fig. 3b). A temperature of 400 °C gave rise to an extremely weak Ms of the prepared catalyst JHC-12–T_2-SO_3H@Fe/Fe_3O_4 of 0.190 A m^2 kg^{-1} after sulfonation for 12 h at 180 °C. When the temperature was increased to 600 °C, the Ms of the prepared catalyst reached a peak value of 40.3 A m^2 kg^{-1}.

The TAC was also affected by the carbonization temperature. In an analysis of the thermal stability of the JHC-12-200@Fe/Fe_3O_4 precursor, a weight loss (of about 6.06 wt%) was observed at 203–400 °C (Fig. S1†), where the loss of C, H and O elements (wt%: C 41.8 *vs.* 36.3, H 4.93 *vs.* 3.97, O 19.6 *vs.* 17.0) was confirmed by elemental analysis (Table S1†). However, the JHC-12-400@Fe/Fe_3O_4 and JHC-12-600@Fe/Fe_3O_4 precursors, which had similar elemental contents (Table S1,† wt%: C 36.3 *vs.* 35.1, H 3.97 *vs.* 3.88, O 17.0 *vs.* 16.2, Fe 40.7 *vs.* 42.9), possessed higher thermal stabilities up to a temperature of 400–601 °C. The weight loss (about 0.90 wt%, Fig. S2†) of the JHC-12-400@Fe/Fe_3O_4 precursor indicated the slight release of volatile compounds from the sample. The significant weight

loss (about 3.06 wt%, Fig. S1†) between 601 and 800 °C could be due to the reaction $C + Fe_3O_4 \rightarrow Fe/Fe_3C + CO_2\uparrow$, with decreases in the C and O contents to 31.6 wt% and 13.4 wt%, respectively. In addition, XRD analysis confirmed the formation of Fe and Fe_3C in the sample (Fig. 5A-a).[28]

Lower temperatures ensured a moderate content of hydrogen and oxygen atoms, which could be bonded by $-SO_3H$ groups on the surface of the precursor.[32] With an excessive carbonization temperature, the loss of active bonding sites for the formation of layers of aromatic carbon on the surface of the precursor would significantly impair the efficiency of sulfonation.[33] With an increase in the carbonization temperature from 400 to 800 °C, the TAC of the catalysts exhibited a dramatic decrease from 3.35 mmol g^{-1} to 1.12 mmol g^{-1}. To achieve a balance between the Ms and TAC, 600 °C was selected as the optimized temperature for the carbonization of the precursor. Under these conditions, the TAC and Ms of the prepared JHC-12-600-SO_3H@Fe/Fe_3O_4 were 2.69 mmol g^{-1} and 40.3 A m^2 kg^{-1}, respectively.

3.2. Characteristics of JHC-12-600@Fe/Fe_3O_4 and JHC-12-600-SO_3H@Fe/Fe_3O_4

3.2.1. XRD and VSM. The XRD pattern of JHC-12-600@Fe/Fe_3O_4 displayed strong signals of a well-crystallized Fe structure (Fig. 5A-a), but the peak intensities for the crystal structures of Fe_3O_4 and Fe_3C were low. This indicated the reduction of Fe_3O_4 to Fe and further to Fe_3C at 600 °C *via* the reactions [$Fe_3O_4 + C \rightarrow Fe + CO_2/CO\uparrow$] and [$Fe + C \rightarrow Fe_3C$].[34,35] The JHC-12-600-SO_3H@Fe/Fe_3O_4 catalyst displayed a distinct diffraction pattern (Fig. 5A-b). The appearance of Fe_2O_3 peaks revealed the occurrence of the reaction [$Fe + H_2SO_4 \rightarrow Fe_2O_3 + H_2O + SO_2\uparrow$] during the sulfonation process. The Fe_2O_3 film could have protected the inner Fe core from further corrosion by H_2SO_4, which led to diminished diffraction peaks of Fe. Moreover, the JHC-12-600-SO_3H@Fe/Fe_3O_4 catalyst also exhibited a strong diffraction peak (at $2\theta = 20–30°$), which demonstrated the presence of aromatic carbon sheets,[26] with a randomly oriented surface of amorphous carbons.[36]

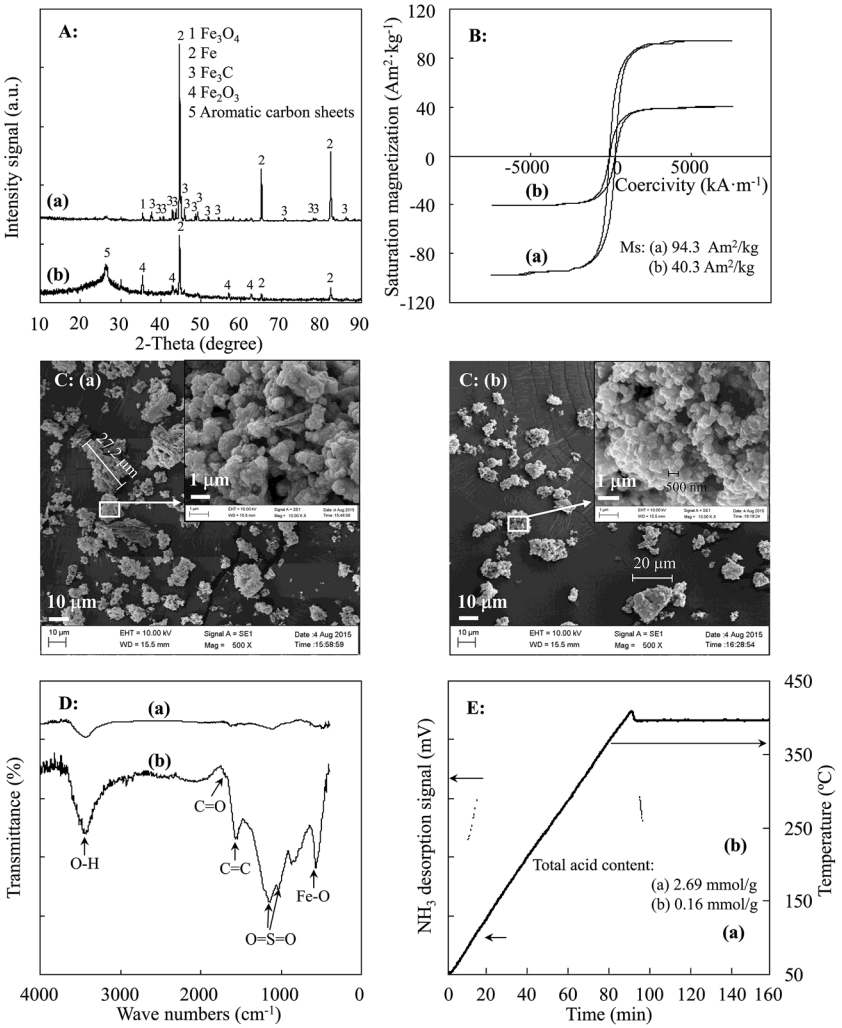

Fig. 5 Characterization of (a) magnetic JHC-12-600@Fe/Fe_3O_4 precursor and (b) magnetic JHC-12-600-SO_3H@Fe/Fe_3O_4 catalyst: (A) XRD, (B) VSM, (C) SEM, (D) FT-IR, and (E) NH_3-TPD.

As magnetic Fe and Fe_3C have a higher magnetic saturation than Fe_3O_4,[37] JHC-12-600@Fe/Fe_3O_4 had a higher magnetic saturation of 94.3 A m^2 kg^{-1} than that of carbonaceous Fe_3O_4 owing to the remarkable conversion of Fe_3O_4 into Fe and Fe_3C.[28] Owing to the loss of Fe_3O_4 and Fe_3C, which was caused by dissolution in the concentrated H_2SO_4 solution, the Ms of JHC-12-600-SO_3H@Fe/Fe_3O_4 declined to 40.3 A m^2 kg^{-1} (Fig. 5B). However, the Ms of JHC-12-600-SO_3H@Fe/Fe_3O_4 was still stronger than that of the AC-600-SO_3H@Fe/C catalyst, which was only 14.4 A m^2 kg^{-1}.[28]

3.2.2. SEM and BET. SEM analysis (Fig. 5C-a) showed small-sized agglomerates of the JHC-12-600@Fe/Fe_3O_4 precursor with smaller rough particles on their surface. This was distinct from the pattern in which AC-600@Fe/C agglomerated in the form of smooth spheres with a size of 50–100 μm in previous works.[28] It was also observed that the JHC-12-600-SO_3H@Fe/Fe_3O_4 catalyst contained agglomerated particles with a better size (<30 μm) (Fig. 5C–b). The size of the particles was smaller than that of the agglomerated AC-600-SO_3H@Fe/C catalyst (50–100 μm). As metal oxides were exposed on the surface of the catalyst precursor without complete coverage by carbonaceous materials, JHC-12-600@Fe/Fe_3O_4 could be corroded internally owing to penetration by H_2SO_4 during sulfonation. Therefore, the size of the JHC-12-600-SO_3H@Fe/Fe_3O_4 particles was slightly reduced (<20 μm), with numerous spherical nanoparticles (size of <500 nm) attached to the surface (Fig. 5C-b). In addition to the change in the morphological pattern, the reduction in particle size and formation of microporous structures, as well as the removal of residual Fe_3C particles from the surface of the precursor contributed to the increase in the surface area and pore volume of the catalyst. Nitrogen adsorption–desorption isotherms are shown in Fig. S2.† In comparison with JHC-12-600@Fe/Fe_3O_4, the specific surface area and pore volume of JHC-12-600-SO_3H@Fe/Fe_3O_4 increased from 23.5 m^2 g^{-1} and 0.048 cm^3 g^{-1} to 46.7 m^2 g^{-1} and 0.093 cm^3 g^{-1}, respectively. Furthermore, it was observed that the sulfonation process could reduce the average pore width from 24.6 nm in the precursor to 8.95 nm in the catalyst. This phenomenon could be explained by (i) the dissolution of Fe_3O_4 and Fe_3C in the JHC-12-600@Fe/Fe_3O_4 precursor by concentrated H_2SO_4 (Fig. 5A-a) and (ii) occupation of the pore volume by newly formed active groups.[28]

3.2.3. FT-IR, elemental analysis and NH_3-TPD. The FT-IR absorption spectra (Fig. 5D) exhibited stretching vibrations of O–H and C=O bonds at 3460 cm^{-1} and 1610 cm^{-1}, respectively, which indicated the presence of –OH and –COOH groups in both JHC-12-600@Fe/Fe_3O_4 and JHC-12-600-SO_3H@Fe/Fe_3O_4.[24] The formation of Fe_2O_3 in JHC-12-600-SO_3H@Fe/Fe_3O_4 was indicated by the Fe–O stretching vibration at 560 cm^{-1}, which was further confirmed by the XRD analysis (Fig. 5A-b). Moreover, the C=C stretching vibration at 1640 cm^{-1} and the C–O–S and O=S=O stretching vibrations at 1054–1060 and 1140–1180 cm^{-1} indicated the introduction of aromatic carbons and –SO_3H groups, respectively, into the JHC-12-600-SO_3H@Fe/Fe_3O_4 catalyst (Fig. 5D-b).[20,28]

The content of sulfonic acid groups (–SO_3H) in the JHC-12-600-SO_3H@Fe/Fe_3O_4 catalyst was 1.13 mmol g^{-1}, as calculated by elemental analysis, which showed a remarkable increase in the S content after sulfonation (Table 2). With the active –SO_3H groups, the TAC of the catalyst reached 2.69 mmol g^{-1}, as determined by NH_3-TPD (Fig. 5E-b). The sulfonation treatment led to an increase of 1680% in the total acidity of JHC-12-600@Fe/Fe_3O_4, in which the original –OH and –COOH[28] groups only displayed an acidity of 0.16 mmol g^{-1}. With its high acidity, JHC-12-600-SO_3H@Fe/Fe_3O_4 could be a favorable candidate as a catalyst for the production of biodiesel from *Jatropha* oil with a high AV.

3.3. Production of *Jatropha* biodiesel with JHC-12-600-SO_3H@Fe/Fe_3O_4

According to previously reported conditions for the production of biodiesel (catalyst loading of 10 wt%, a molar ratio of methanol/oil of 24/1, a reaction temperature of 200 °C and a reaction time of 10 h),[28] optimization of the catalyst dosage (2.5–12.5 wt% with respect to *Jatropha* oil), molar ratio of methanol to oil (6/1–30/1), reaction temperature (180–220 °C) and reaction time (2.5–12.5 h) for the production of *Jatropha* biodiesel was performed by single-factor tests. Each run was duplicated and the average values of the results were reported (Fig. 6).

3.3.1. Methanol/oil molar ratio. Although a theoretical molar ratio of methanol/oil (MOR) of 3/1 has been proposed for the transesterification of triglycerides, higher MORs ranging from 6/1 to 30/1 have been widely used for reactions at high temperatures owing to extensive evaporation of methanol into the dead volume of the reactor.[28] Fig. 6A-a shows that the biodiesel yield rapidly increased from 39.6% to 81.7% when the MOR increased from 6/1 to 12/1. The biodiesel yield reached a peak value of 94.2% at an MOR of 24/1. A great increase in the ratio to 30/1 led to a slight decline in the biodiesel yield to 92.7%, as the excessive mass of methanol reduced the relative concentration of the catalyst in the reaction mixture.[28]

When the catalyst was reused, the biodiesel yield increased from 33.0% to a maximum value of 88.5% with an increase in the MOR from 6/1 to 18/1 (Fig. 6A-b). However, increases in the MOR to 24/1 and further to 30/1 led to declines in the biodiesel yield to 85.5% and 82.1%, respectively. A similar effect of an increase in MORs on changes in the biodiesel yield was revealed using either fresh or recycled catalysts. As the pore structures in magnetic JHC-12-600-SO_3H@Fe/Fe_3O_4 could be filled with methanol, the decline in the biodiesel yield was possibly due to a relatively low catalyst concentration that was caused by the higher MOR in the reaction system.[28] Therefore, 18/1 was selected as the optimum MOR in the following experiments.

3.3.2. Catalyst loading. A catalyst loading of 2.5 wt% to 12.5 wt% with an MOR of 18/1 was employed at 200 °C for 10 h. The catalyst loading obviously affected the biodiesel yield when the fresh catalyst was used. With an increase in the catalyst loading from 2.5 to 7.5 wt%, the biodiesel yield increased from 66.5% to 94.6% (Fig. 6B-a). Further increases in the catalyst loading to 10 and 12.5 wt% led to a slight decrease in the biodiesel yield from 94.1% to 91.8% owing to poor distribution of the catalyst at high concentrations by magnetic stirring within a limited volume.[28]

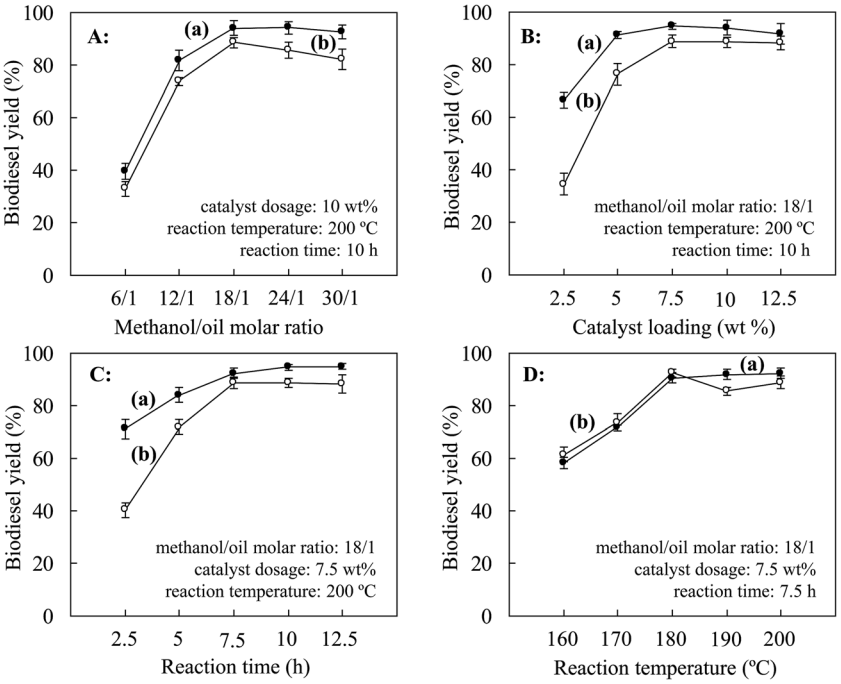

Fig. 6 Single-factor optimization of production of biodiesel from *Jatropha* oil with the magnetic JHC-12-600-SO_3H@Fe/Fe_3O_4 catalyst used for (a) 1 and (b) 2 cycles: (A) methanol/oil molar ratio, (B) catalyst loading, (C) reaction time, and (D) reaction temperature.

The catalyst loading with the fresh catalyst and with the recycled catalyst displayed remarkable differences in their effect on the biodiesel yield. With a loading of 2.5 wt% of the fresh catalyst and when the catalyst had been used once, the biodiesel yield was 66.5% and 34.6%, respectively (Fig. 6B-a and b). Increases in the catalyst loading to 5, 7.5, 10.0 and 12.5 wt% gradually narrowed the gap between the catalysts to 14.9%, 5.8%, 5.6% and 3.5%, respectively. To limit the cost by reducing the catalyst loading, 7.5 wt% was selected as the optimum level of catalyst loading.

3.3.3. Reaction time. Under conditions of an MOR of 18/1, a catalyst loading of 7.5 wt% and a reaction temperature of 200 °C, the biodiesel yield underwent a significant increase between reaction times of 2.5 and 7.5 h and reached a maximum value of 94.8% with the fresh catalyst after 12.5 h (Fig. 6C-a). Reuse of the catalyst caused a reduction in the biodiesel yield, owing to the loss of part of the active groups (Fig. 6C-b).[28] However, the difference in biodiesel yield between the fresh and recycled catalysts decreased with an increase in the reaction time. A time of 7.5 h was selected as the optimum reaction time, with a reduction in efficiency of only 5.8% when the recycled catalyst was used.

3.3.4. Reaction temperature. Five reaction temperatures of between 160 and 200 °C were tested (Fig. 6D). When the fresh catalyst was used, a remarkable increase in the biodiesel yield from 58.3% to 90.6% occurred between 160 and 180 °C. The biodiesel yield reached 92.0% at 190 °C and increased slightly to 92.4% at 200 °C (Fig. 6D-a).

When the catalyst was reused, a similar trend of an increase in the biodiesel yield from 61.5% to 92.5% was achieved as the temperature was increased from 160 to 180 °C (Fig. 6D-b). However, with further increases in the temperature to 190 °C and 200 °C, the biodiesel yield declined to 85.6% and 88.8%, respectively, but was slightly promoted at the higher reaction temperature of 200 °C *via* a change in the chemical equilibrium of the transesterification reactions.[28] This indicated that firmly bonded active –SO_3H groups on the fresh catalyst remained when the temperature was lower than 180 °C, at which sulfonation and hydrothermal pretreatment were performed on the catalyst.[28] Higher temperatures could cause a slight deactivation of the catalyst by releasing part of the active groups. Therefore, 180 °C was selected as the optimum operating temperature of the catalyst.

3.4. Performance of magnetic JHC-12-600-SO_3H@Fe/Fe_3O_4 catalyst in scaled-up applications

To evaluate the feasibility of using the magnetic JHC-12-600-SO_3H@Fe/Fe_3O_4 catalyst for practical applications, the scaled-up production of *Jatropha* biodiesel was performed with an MOR of 18/1 and a catalyst loading of 7.5 wt% in a 5 L batch reactor (Fig. 2) at 180 °C for 7.5 h. Under optimal conditions, the JHC-12-600-SO_3H@Fe/Fe_3O_4 catalyst was reused for 5 cycles with an average recovery rate of 94.3 ± 1.8 wt%. The biodiesel yield was 96.5%, 97.4%, 96.7%, 95.6% and 93.2%, respectively, whereas AV values of 0.25, 0.19, 0.27, 0.36 and 0.38 mg KOH per g were achieved after the first to fifth reaction cycles (Fig. 7). An average biodiesel yield of 95.9% and an AV of 0.29 mg KOH per g were achieved, which were slightly lower than the international standards for biodiesel products (96.5% and 0.5 mg KOH per g), respectively.[38] The biodiesel yield reached 93.2% when the catalyst was reused for the fifth time. In comparison to 96.5%, which was the biodiesel yield with the new catalyst, the decline was considered to be due to the leaching of –SO_3H

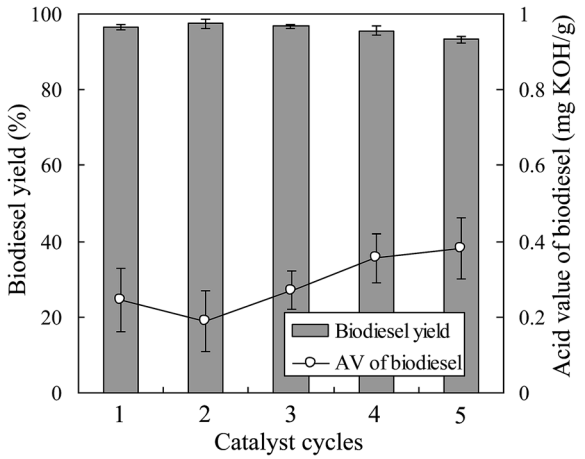

Fig. 7 Reuse of the JHC-12-600-SO_3H@Fe/Fe_3O_4 catalyst for the production of *Jatropha* biodiesel in a 5 L batch reactor (reaction conditions: 180 °C for 7.5 h with a methanol/oil molar ratio of 18/1 and a catalyst loading of 7.5 wt%).

groups from the catalyst. On the basis of the reduction in the sulfur content from 3.62 to 2.37 wt% (Table 2), the calculated leaching rate of –SO_3H groups was 34.5% on the assumption that all the sulfur atoms were associated with sulfonic acid groups.[27,28]

The scaled-up experiments resulted in much higher biodiesel yields than those achieved in the 50 mL batch reactor (96.5% and 97.4% *vs.* 90.6% and 92.5% when the catalyst was used twice). This may have been caused by the difference in efficiency when mixing the catalysts with methanol and oil between agitator blades and magnetic stirrers (Fig. 2a *vs.* Fig. 1c). In comparison with the previous work,[28] higher biodiesel yields were achieved (90.6% and 92.5% *vs.* 90.5% and 91.8% for 2 reaction cycles) when the JHC-12-600-SO_3H@Fe/Fe_3O_4 catalyst was employed in the 50 mL batch reactor under much milder optimum conditions (*vs.* an MOR of 24/1 and a catalyst loading of 10 wt% at 200 °C for 10 h). In addition, the Ms of the JHC-12-600-SO_3H@Fe/Fe_3O_4 catalyst was much higher than that of AC-600-SO_3H@Fe/C (40.3 *vs.* 14.4 A m^2 kg^{-1}), as was previously reported. A catalyst with a strong Ms would be more suitable for use in a scaled-up reactor, because its strong attraction to an NdFeB magnet will prevent it from being carried out by the discharged biodiesel product (Fig. 2).

With high values of TAC and Ms, JHC-12-600-SO_3H@Fe/Fe_3O_4 displayed better performance in the direct production of biodiesel (Table 1). Moreover, this also indicates that JHC-12-600-SO_3H@Fe/Fe_3O_4 potentially has high efficiency in the esterification of free fatty acids at low temperatures (<100 °C).[22] Therefore, it could be combined with solid bases in the production of biodiesel from crude oils with a high AV *via* a two-process conversion method.[39]

4. Conclusions

Magnetic carbonaceous acids derived from hydrolysates of *Jatropha* hulls were successfully synthesized. The JHC-12-600-SO_3H@Fe/Fe_3O_4 catalyst, which contained coating layers of aromatic carbon bonded to abundant active groups (–OH, –COOH and –SO_3H), possessed a high TAC and Ms (2.69 mmol g^{-1} and 40.3 A m^2 kg^{-1}). It displayed high activity and stability in the direct catalysis of the transesterification of *Jatropha* oil with a high AV (17.2 mg KOH per g) for the production of biodiesel. In a 5 L batch reactor, JHC-12-600-SO_3H@Fe/Fe_3O_4 could be effectively recycled by a magnet for direct reuse. An average biodiesel yield of 95.9% was achieved after 5 reaction cycles with a catalyst recovery rate of 94.3%. Owing to their stable performance and multiple potential applications, the synthesis of magnetic carbonaceous acids derived from the hydrolysates of *Jatropha* hulls enabled the green and economic utilization of energy plant waste in the co-production of biodiesel products.

Acknowledgements

The authors wish to acknowledge the financial support from the Youth Innovation Promotion Association CAS (No. 2017440) and Natural Science Foundation of China (No. 31400518).

References

1 M. Z. Jacobson, *Energy Environ. Sci.*, 2009, **2**, 148–173.
2 Z. Y. Hua, P. Q. Tan, X. Y. Yan and D. M. Lou, *Energy*, 2008, **33**, 1654–1658.
3 L. Lin, C. S. Zhou, V. Saritporn, X. Q. Shen and M. D. Dong, *Appl. Energy*, 2011, **88**, 1020–1031.
4 E. Lois, *Fuel*, 2007, **86**, 1212–1213.
5 Q. Kwok, B. Acheson, R. Turcotte, A. Janès and G. Marlair, *J. Therm. Anal. Calorim.*, 2013, **111**, 507–515.
6 V. Mutreja, S. Singh, T. K. Minhas and A. Ali, *RSC Adv.*, 2015, **5**, 46890–46896.
7 S. B. Chavan, R. R. Kumbhar, D. Madhu, B. Singh and Y. C. Sharma, *RSC Adv.*, 2015, **5**, 63596–63604.
8 S. Sharma, D. Medpelli, S. J. Chen and D. K. Seo, *RSC Adv.*, 2015, **5**, 65454–65461.
9 J. C. Juan, D. A. Kartika, T. Y. Wu and T. Y. Y. Hin, *Bioresour. Technol.*, 2011, **102**, 452–460.
10 H. C. Ong, A. S. Silitonga, H. H. Masjuki, T. M. I. Mahlia, W. T. Chong and M. H. Boosroh, *Energy Convers. Manage.*, 2013, **73**, 245–255.
11 M. Y. Koh and T. I. M. Ghazi, *Renewable Sustainable Energy Rev.*, 2011, **15**, 2240–2251.
12 S. Jain and M. P. Sharma, *Energy*, 2011, **36**, 5409–5415.
13 F. Zhang, Z. Fang and Y. T. Wang, *Fuel*, 2015, **150**, 370–377.
14 W. J. Li, Y. J. Gao, S. Y. Yao, D. Ma and N. Yan, *Green Chem.*, 2015, **17**, 4198–4205.
15 B. Norjannah, H. C. Ong, H. H. Masjuki, J. C. Juan and W. T. Chong, *RSC Adv.*, 2016, **6**, 60034–60055.
16 R. Hou, D. Zhang, X. Duan, X. Wang, S. Wang and Z. Sun, *RSC Adv.*, 2016, **6**, 81794–81801.
17 A. S. Badday, A. Z. Abdullah and K. T. Lee, *Renewable Energy*, 2013, **50**, 427–432.
18 J. M. Rafi, A. Rajashekar, M. Srinivas, B. V. S. K. Rao, R. B. N. Prasad and N. Lingaiah, *RSC Adv.*, 2015, **5**, 44550–44556.

19 T. C. Su, Z. Fang, F. Zhang, J. Luo and X. K. Li, *Sci. Rep.*, 2015, **5**, 17538–17542.
20 E. L. S. Ngee, Y. J. Gao, X. Chen, T. M. Lee, Z. G. Hu, D. Zhao and N. Yan, *Ind. Eng. Chem. Res.*, 2014, **53**, 14225–14233.
21 H. C. Ong, A. S. Silitonga, H. H. Masjuki, T. M. I. Mahlia, W. T. Chong and M. H. Boosroh, *Energy Convers. Manage.*, 2013, **73**, 245–255.
22 F. L. Pua, Z. Fang, S. Zakaria, C. H. Chia and F. Guo, *Biotechnol. Biofuels*, 2011, **4**, 56–64.
23 H. Cui, S. Q. Turn and M. A. Reese, *Catal. Today*, 2009, **139**, 274–279.
24 L. Hu, X. Tang, Z. Wu, L. Lin, J. Xu, N. Xu and B. Dai, *Chem. Eng. J.*, 2015, **263**, 299–308.
25 Z. Liu, X. Fu, S. Tang, Y. Cheng, L. Zhu, L. Xing, J. Wang and L. Xue, *Catal. Commun.*, 2014, **56**, 1–4.
26 C. Zhang, H. Wang, F. Liu, L. Wang and H. He, *Cellulose*, 2013, **20**, 127–134.
27 H. X. Guo, Y. F. Lian, L. L. Yan, X. H. Qi and R. L. Smith Jr, *Green Chem.*, 2013, **15**, 2167–2174.
28 F. Zhang, Z. Fang and Y. T. Wang, *Appl. Energy*, 2015, **155**, 637–647.
29 K. Nakajima and M. Hara, *J. Am. Ceram. Soc.*, 2007, **90**, 3725–3734.
30 F. Zhang, X. H. Wu, M. Yao, Z. Fang and Y. T. Wang, *Green Chem.*, 2016, **18**, 3302–3314.
31 B. J. Xue, J. Luo, F. Zhang and Z. Fang, *Energy*, 2014, **68**, 584–591.
32 J. M. Anderson, R. L. Johnson, K. Schmidt-Rohr and B. H. Shanks, *Carbon*, 2014, **74**, 333–345.
33 L. Wang, X. Dong, H. Jiang, G. Li and M. Zhang, *Bioresour. Technol.*, 2014, **158**, 392–395.
34 M. C. Pereira, F. S. Coelho, C. C. Nascentes, J. D. Fabris, M. H. Araújo, K. Sapag, L. C. A. Oliveira and R. M. Lago, *Chemosphere*, 2010, **81**, 7–12.
35 Y. Fei and E. Brosh, *Earth Planet. Sci. Lett.*, 2014, **408**, 155–162.
36 F. A. Dawodu, O. Ayodele, J. Xin, S. Zhang and D. Yan, *Appl. Energy*, 2014, **114**, 819–826.
37 R. López de Arroyabe Loyo, S. I. Nikitenko, A. C. Scheinost and M. Simonoff, *Environ. Sci. Technol.*, 2008, **42**, 2451–2456.
38 M. Oguma, Y. J. Lee and S. Goto, *Int. J. Automot. Tech.*, 2012, **13**, 33–41.
39 P. M. Guo, F. H. Huang, M. M. Zheng, W. L. Li and Q. D. Huang, *J. Am. Oil Chem. Soc.*, 2012, **89**, 925–933.